Preclinical Development

Molecular Cancer Therapeutics

A Locked, Dimeric CXCL12 Variant Effectively Inhibits Pulmonary Metastasis of CXCR4-Expressing Melanoma Cells Due to Enhanced Serum Stability

Tomonori Takekoshi[1], Joshua J. Ziarek[2], Brian F. Volkman[2], and Sam T. Hwang[1]

Abstract

The CXC chemokine receptor-4 (CXCR4) plays a critical role in cancer by positively regulating cancer cell metastasis and survival. We previously showed that high concentrations of the CXCR4 ligand, wild-type CXCL12 (wtCXCL12), could inhibit colorectal cancer metastasis *in vivo*, and we have hypothesized that wtCXCL12 dimerizes at high concentration to become a potent antagonist of CXCR4. To address this hypothesis, we engineered a covalently locked, dimeric variant of CXCL12 (CXCL122). Herein, we show that CXCL122 can not only inhibit implantation of lung metastasis of CXCR4-B16-F10 melanoma cells more effectively than AMD3100, but that CXCL122 also blocks the growth of established pulmonary tumors. To identify a basis for the *in vivo* efficacy of CXCL122, we conducted Western blot analysis and ELISA analyses, which revealed that CXCL122 was stable for at least 12 hours in serum, whereas wtCXCL12 was quickly degraded. CXCL122 also maintained its antagonist properties in *in vitro* chemotaxis assays for up to 24 hours in serum, whereas wtCXCL12 was ineffective after 6 hours. Heat-inactivation of serum prolonged the stability and function of wtCXCL12 by more than 6 hours, suggesting enzymatic degradation as a possible mechanism for wtCXCL12 inactivation. *In vitro* analysis of amino-terminal cleavage by enzymes dipeptidylpeptidase IV (DPPIV/CD26) and matrix metalloproteinase-2 (MMP-2) resulted in 25-fold and 2-fold slower degradation rates, respectively, of CXCL122 compared with wtCXCL12. In summary, our results suggest CXCL122 possesses greater potential as an antimetastatic drug as compared with AMD3100 or wtCXCL12, potentially due to enhanced serum stability in the presence of N-terminal degrading enzymes. *Mol Cancer Ther; 11(11); 2516–25. ©2012 AACR.*

Introduction

Cancer metastasis to vital organs represents the major source of mortality in cancer. Metastasis is a complex process that is dependent upon many factors, including tumor cell properties, the tumor microenvironment, and host tumor immunity. Chemokine signaling plays a crucial role in cancer metastasis, neoangiogenesis, and proliferation as well as infiltration of tumor-associated immune cells (1, 2). We have focused on CXC chemokine receptor-4 (CXCR4), which is upregulated in at least 23 different cancers (3). We previously showed that CXCR4 enhances β1 integrin-dependent pulmonary metastasis of B16 melanoma cells 6- to 10-fold following intravenous inoculation (4, 5). We also showed that T22, a specific CXCR4 inhibitor, effectively blocked pulmonary dissemination of CXCR4-expressing B16 cells following tail vein inoculation (4), suggesting that blocking CXCR4 may be an effective strategy for preventing lung metastasis.

Recently, we reported that exogenous administration of CXCL12, the ligand of CXCR4, inhibits colorectal cancer metastasis (6). CXCL12 exists in a monomer–dimer equilibrium in which both states bind CXCR4 and stimulate a calcium response, but only the monomeric variant promotes cell migration (7, 8). We previously engineered a covalently locked, dimeric variant of CXCL12 ($CXCL12_2$; ref. 8) and showed that intraperitoneal administration inhibited the metastasis of CXCR4-overexpressing colon cancer cells to the liver (6). $CXCL12_2$ was a more potent inhibitor of colorectal metastasis than wtCXCL12. Concurrently, $CXCL12_2$ diminished pulmonary implantation following tail vein injection of B16 melanoma cells (6). WtCXCL12, however, exhibits a half-life on the order of minutes (9) and is degraded by numerous enzymes, including matrix metalloproteinase-2 (MMP-2; ref. 10) and dipeptidylpeptidase IV (DPPIV/CD26; ref. 11), which may render wtCXCL12 a poor choice as a therapeutic inhibitor of CXCR4.

Authors' Affiliations: Departments of [1]Dermatology and [2]Biochemistry, Medical College of Wisconsin and Froedtert Hospital, Milwaukee, Wisconsin

Note: Supplementary data for this article are available at Molecular Cancer Therapeutics Online (http://mct.aacrjournals.org/).

Corresponding Author: Sam T. Hwang, Department of Dermatology, Medical College of Wisconsin, FEC 4100, 9200 W. Wisconsin Ave, Milwaukee, WI 53226. Phone: 414-955-3104; Fax: 414-955-6221; E-mail: sthwang@mcw.edu

doi: 10.1158/1535-7163.MCT-12-0494

©2012 American Association for Cancer Research.

Downloaded from http://aacrjournals.org/mct/article-pdf/11/11/2516/2320571/2516.pdf by guest on 15 January 2025

Herein, we show that intravenous $CXCL12_2$ treatment inhibited initial pulmonary dissemination of CXCR4-expressing B16 more effectively than the U.S. Food and Drug Administration (FDA)-approved CXCR4 inhibitor, AMD3100. Importantly, $CXCL12_2$ also inhibited the growth of established CXCR4-expressing B16 lung metastatic tumors, suggesting that it may have utility in treating established metastasis in humans. $CXCL12_2$ was much more stable than wtCXCL12 in mouse serum, maintaining its inhibitory function in chemotaxis assays for at least 12 hours. $CXCL12_2$ showed enhanced stability in the presence of DPPIV/CD26 and MMP-2 N-terminal degrading enzymes, which likely contributed to the superior activity of $CXCL12_2$ in the presence of mouse serum. These data suggest that $CXCL12_2$ has a potential for clinical use in the treatment of metastatic tumors.

Materials and Methods

Animals and cell lines

Female C57BL/6 mice (8–12 weeks old) were purchased from Charles River Laboratories or The Jackson Laboratory and used in accordance with the guidelines of the Animal Use and Care Committee of the Medical College of Wisconsin. B16-F10 melanoma cells are a kind gift from Dr. Kiyoshi Ariizumi (Dermatology, UT Southwestern Medical Center, Dallas, TX; ref. 12). Syngeneic B16-F1 melanoma cells (originally obtained from the NCI-Frederick Cancer Research and Development Center) and B16-F10 melanoma cells were grown in Dulbecco's Modified Eagle's Media (Invitrogen) with 10% heat-inactivated FBS and supplements as previously described (13). Neither the B16-F10 melanoma cell line nor the B16-F1 melanoma cell line have been authenticated since acquisition, although both produce melanin pigment as expected for melanoma cell lines. THP-1 cells were obtained from American Type Culture Collection but have not been authenticated since acquisition.

Retroviral transduction of B16-F1 and B16-F10 melanoma cells

Human CXCR4 cDNA (14), a gift from Dr. E. Berger (National Institute of Allergy and Infectious Diseases, Bethesda, MD), was subcloned into the pLNCX2 retroviral vector (Clontech). Using this vector, B16-F1 melanoma cells and B16-F10 cells were transduced as previously described (13) to yield CXCR4-B16 cells.

Construction of plasmids

Human CXCL12 and $CXCL12_2$ were cloned from the previously described pQE30 vectors (7, 8) into a pET28a vector that incorporates a N-terminal His_6 and *Saccharomyces cerevisiae* SUMO protein (Smt3). The final, purified CXCL12 protein constructs possess a native N-terminal sequence for proper function. All expression vector inserts were confirmed by DNA sequencing.

Protein expression and purification

Smt-CXCL12 expression vectors were transformed into *Escherichia coli* strain BL21 (DE3), and cells were grown at 37°C in Luria-Bertani medium. Protein expression was induced by the addition of isopropyl-β-D-thiogalactopyranoside to a final concentration of 1 mmol/L when the culture reached an OD_{600} of 0.6. After incubation at 37°C for 6 hours, cells were pelleted at 5,000 × *g* and stored at −80°C until further processing. Cell pellets were resuspended in 10 mL of a buffer containing 50 mmol/L Na_2PO_4 (pH 8.0), 300 mmol/L NaCl, 10 mmol/L imidazole, 1 mmol/L phenylmethylsufonyl fluoride, and 0.1% (v/v) 2-mercaptoethanol. Resuspended cells were lysed by 3 passages through a French press. Inclusion bodies were collected by centrifugation at 15,000 × *g*, and the supernatant was discarded. The insoluble inclusion body pellet was dissolved in buffer AD [6 mol/L guanidinium chloride, 50 mmol/L Na_2PO_4 (pH 8.0), 300 mmol/L NaCl, 10 mmol/L imidazole] and batch loaded onto 2 mL of Ni-NTA resin (Qiagen). After 30 minutes the column was washed with 4 × 10 mL of buffer AD followed by elution with a buffer containing 6 mol/L guanidinium chloride, 50 mmol/L sodium acetate (pH 4.5), 300 mmol/L NaCl, and 10 mmol/L imidazole. The eluate was pooled and refolded via dropwise dilution into a 20 mmol/L Tris (pH 8.0), 10 mmol/L cycteine, and 0.5 mmol/L cystine solution. Following overnight refolding, the solution was concentrated by ultrafiltration (MWCO 10 kDa), and the tag cleaved by incubation with 500 μg Ulp1 protease at 30°C for 12 hours. The Smt-tag was separated from the protein using cation-exchange chromatography. Samples were batch loaded onto SP Sepharose Fast Flow resin (GE Healthcare UK Ltd.) and washed with Tris (pH 8.0), 50 mmol/L NaCl to remove the Smt-tag. Protein was eluted with 20 mmol/L Tris (pH 8.0) containing 2 mol/L NaCl. Finally, samples were purified to more than 98% homogeneity using reverse-phase high-performance liquid chromatography with a 30-minute gradient from 30% to 60% ACN in aqueous 0.1% trifluoroacetic acid. CXCL12 variants were frozen, lyophilized, and stored at −20°C. Purity, identity, and molecular weight were verified by matrix-assisted laser desorption ionization time-of-flight (MALDI-TOF) mass spectrometry and nuclear magnetic resonance spectroscopy.

Inoculation of transduced cell lines

CXCR4-B16 and pLNCX2-B16 cells in exponential growth phase were harvested and washed 2 times in PBS before injection. Cell viability was more than 90% as determined by trypan blue dye exclusion. For intravenous injection, 4×10^5 CXCR4-B16 or pLNCX2-B16 cells in 200 μL were injected into the tail veins of mice. Images are representative of experimental trends.

Luciferase assay

Luciferase activity was measured using a luciferase reporter assay system (Promega). Lungs from each animal were homogenized in 1 mL of lysis buffer, of which 100 μL

Downloaded from http://aacrjournals.org/mct/article-pdf/11/11/2516/2320571/2516.pdf by guest on 15 January 2025

aliquots were then assayed in triplicate. Means of triplicates were used to represent the luciferase activity for a given tissue from a particular animal. Four to 7 animals per experimental treatment group were used in each experiment.

Transwell chemotaxis assay

Chemotaxis was assessed using Costar Transwell migration chambers (5-μm pore; Corning). THP-1 cells were washed with PBS and migration buffer [RPMI 1640 containing 2 mg/mL of bovine serum albumin (BSA)]. Cells [5×10^5 in 100 μL of 1% mouse serum (Sigma) containing migration buffer] were placed in the top well and migration buffer containing 1% mouse serum (Sigma) and the indicated chemokine concentration was added to the bottom wells. Plates were incubated for 3 hours at 37°C and 5% CO_2. Transwell inserts were then removed and cells that had migrated into the lower chamber were counted with a hematocytometer. Migration buffer containing 1% mouse serum was used as a negative control in measuring chemokinesis and basal migration. The chemotactic index was computed as the number of cells that migrated in response to chemokine divided by the number of cells that migrated in the absence of chemokine.

ELISA

A human CXCL12/SDF-1 ELISA kit was purchased from R&D Systems and was used for measuring wtCXCL12 or $CXCL12_2$ concentration in mouse serum (Sigma) following manufacturer's protocol.

Western blotting

Mouse serum samples containing wtCXCL12 or $CXCL12_2$ were loaded onto 4% to 20% Mini-Protean TGX gel (Bio-Rad) and transferred to nitrocellulose membranes (Bio-Rad). Membranes were blocked with 5% BSA (Sigma) for 1 hour and incubated with anti-CXCL12 antibody for CXCL12 ELISA detection antibody (R&D) at 1:500 dilutions for overnight. Membranes were then washed 3 times and incubated with Precision Protein StrepTactin–HRP Conjugate (Bio-Rad) for 1 hour. After washing, membranes were incubated with chemiluminescent solution (ECL Western Blotting Detection Reagents; GE Healthcare UK Ltd.) for 5 minutes at room temperature. Images were acquired and quantified using a ChemiDoc XRS+ system (Bio-Rad).

Calcium flux assay

CXCR4-B16-F10 cells (2×10^5) were harvested, washed by PBS 2 times, and resuspended in 96-well white-walled plates (BD Biosciences Discovery Labware). FLIPR Calcium 4 Assay Kit (Molecular Devices) diluted in HEPES Buffered Saline Solution (HBSS) supplemented with 20 mmol/L HEPES buffer and 0.1% (w/v) BSA was added to the plate as per manufacturer's instructions. For inhibition experiments, cells were additionally treated with 5 μmol/L AMD3100. Plates were centrifuged at $200 \times g$ for 5 minutes and then were incubated in 37°C for 30 minutes. CXCL12 variants were diluted in HBSS/HEPES buffer and added to each well for a 500 nmol/L final concentration. Calcium response was measured by fluorescence spectroscopy every 1.5 seconds for a total of 180 seconds using a FlexStation 3 Microplate Reader (Molecular Devices). Baseline fluorescence was measured 30 seconds before addition of ligand. Values were subsequently normalized to the average baseline fluorescence. Experiments were recorded in quadruplicate on 2 separate days.

DPPIV/CD26 degradation assay

Recombinant human DPPIV/CD26 was purchased from R&D Systems. Degradation reactions ($n = 3$) were composed of 0.2 ng/μL DPPIV/CD26, 10 μmol/L wtCXCL12 (or 5 μmol/L $CXCL12_2$), 2 μmol/L Smt3, and 25 mmol/L Tris (pH 8). At the indicated time points, 1 μL aliquots were quenched with 4 μL sinapinic acid solution and spotted on a MALDI plate. Five spectra, each composed of 100 laser shots, were collected using a Voyager-DE Pro MALDI-TOF spectrometer (PerSeptive Biosystems) for each sample. The intensity of full-length CXCL12 or $CXCL12_2$ was normalized to the Smt3 internal standard. Sample half-life was then calculated using nonlinear regression (Pro Fit).

MMP-2 degradation assay

Recombinant human MMP-2 was purchased from R&D Systems. MMP2 was activated by incubation with 1 mmol/L *p*-aminophenylmercuric acetate in TCNB buffer [50 mmol/L Tris (pH 7.4), 10 mmol/L $CaCl_2$, 150 mmol/L NaCl, and 0.05% (w/v) Brij 35] for 1 hour at 37°C. Reaction samples ($n = 3$) were composed of 1.4 ng/μL MMP-2 and 10 μmol/L Smt-wtCXCL12 (or 5 μmol/L Smt-$CXCL12_2$) in TCNB buffer. At the indicated time points, aliquots were quenched by mixing 1:1 with protein loading buffer and heating to 95°C for 5 minutes. Samples were then stored at −20°C. Before SDS-PAGE, samples were mixed with 1.46 mol/L 2-mercaptoethanol and heated to 95°C for 5 minutes. SDS-PAGE was conducted on a 15% acrylamide gel, and bands were visualized by Coomassie Blue stain. Bands were quantified using a ChemiDoc XRS Molecular Imager (BioRad), and data were fitted to a half-life equation using nonlinear regression (Pro Fit).

Statistical analysis

An unpaired, 2-tailed Student *t* test was used to analyze the results and a $P < 0.05$ was considered statistically significant. All the shown values represent means and *SD*.

Results

$CXCL12_2$ is a more effective inhibitor of lung metastasis than AMD3100

We previously showed that $CXCL12_2$ is an effective inhibitor of CXCR4-B16-F1 cell lung implantation (6). Herein, we used the more tumorigenic B16-F10 cell line that was transduced with CXCR4 (referred to as CXCR4-

Downloaded from http://aacrjournals.org/mct/article-pdf/11/11/2516/2320571/2516.pdf by guest on 15 January 2025

B16-F10). CXCR4-B16-F10 cells (4×10^5 cells/200 μL including drug) were preincubated with various concentrations of $CXCL12_2$, wtCXCL12, or AMD3100 and injected intravenously into the tail veins of female C57BL/6 mice (Fig. 1A). An equivalent dose of $CXCL12_2$, wtCXCL12, or AMD3100 was administered the following day. As shown in Fig. 1B, treatment with either 0.5 μmol/L or 5 μmol/L $CXCL12_2$ strongly inhibited CXCR4-B16-F10 lung metastasis. In contrast, although wtCXCL12 exhibited a dose–response trend, it was unable to significantly prevent CXCR4-B16-F10 lung metastasis (Fig. 1C). We next compared the effectiveness of $CXCL12_2$ with AMD3100, an FDA-approved CXCR4-antagonist in clinical use for stem-cell mobilization (15–17). Neither the equivalent molar concentration (5 μmol/L, 200 μL) nor mass weight (15.9 μg/200 μL; 100 μmol/L) of AMD3100

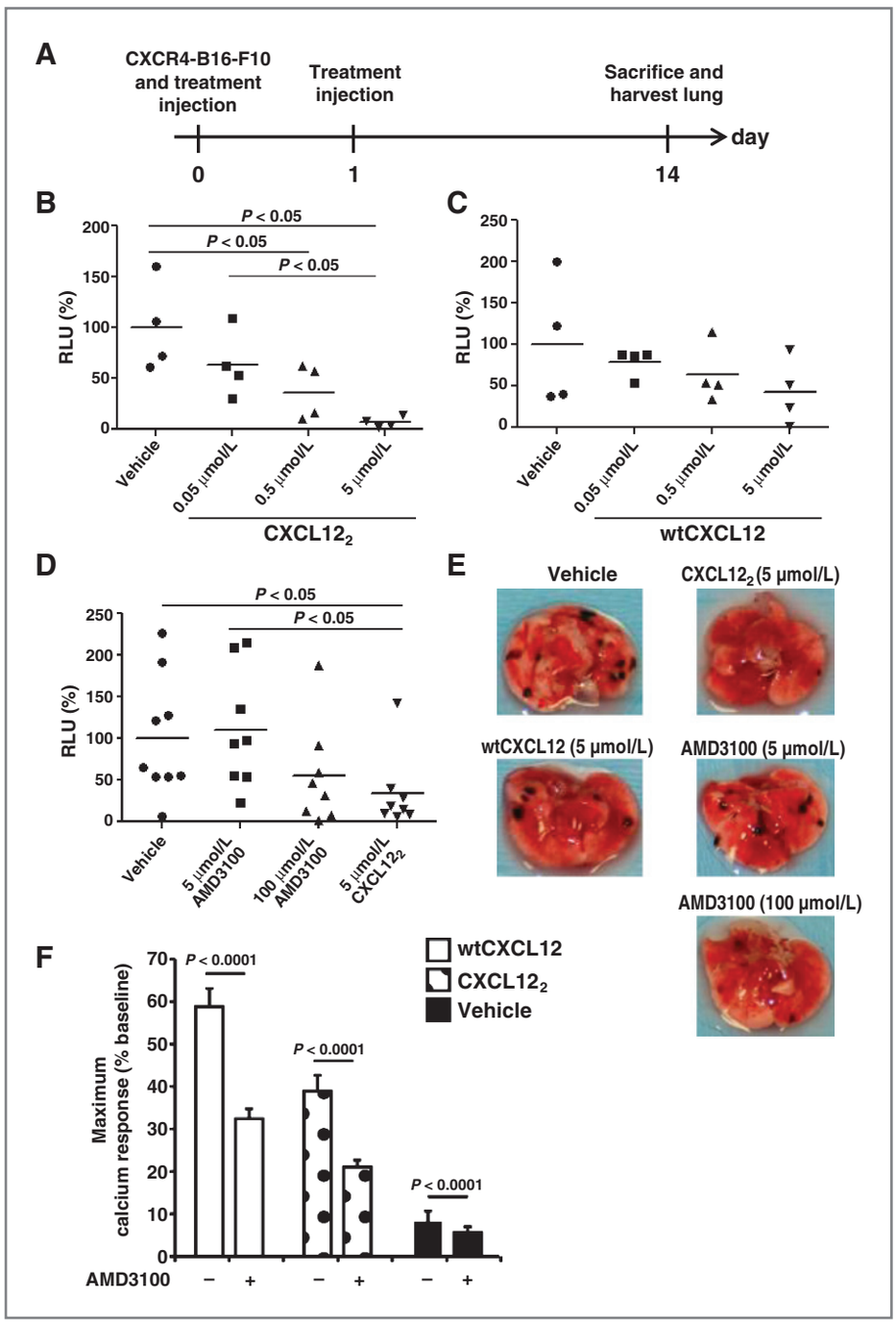

Figure 1. CXCL122 inhibits CXCR4-B16 metastasis more effectively than wtCXCL12 and AMD3100. A, CXCR4-luc-B16-F10 cells (4×10^5) were injected intravenously into the tail vein of C57BL/6 mouse with the indicated concentrations of drugs. On day 1, the animals were given the same treatment intravenously. Lungs were harvested 14 days after inoculation, and luciferase activity was measured to evaluate metastatic tumor. $CXCL12_2$ ($n = 4$; B), wtCXCL12 ($n = 4$; C), and AMD3100 data (vehicle, $n = 9$; others, $n = 8$; data are a summation of 2 independent experiments; D) are shown. E, representative lung images from mice treated with each drug are shown. F, calcium response of CXCR4-luc-B16-F1 cells induced by 500 nmol/L $CXCL12_2$ or wtCXCL12 was measured in the presence and absence of 5 μmol/L AMD3100. Experiments were recorded in quadruplicate on 2 separate days. Tumor burden was assessed by measuring luciferase-dependent light production using relative light units (RLU).

Downloaded from http://aacrjournals.org/mct/article-pdf/11/11/2516/2320571/2516.pdf by guest on 15 January 2025

(MW; 794.47 Da) to 5 μmol/L of $CXCL12_2$ (MW; 15,962 Da) significantly reduced CXCR4-B16-F10 lung metastasis (Fig. 1D). A macroscopic comparison of lung metastases in the presence of these CXCR4 inhibitors is depicted in Fig. 1E. We also measured $CXCL12_2$ inhibition of metastasis using the less tumorigenic B16-F1 cells. We found that 0.5 μmol/L, but not 0.05μmol/L, of $CXCL12_2$ inhibited enhanced CXCR4-B16-F1 lung metastasis and that this dose of $CXCL12_2$ did not affect the lower lung metastasis rates of CXCR4-negative pLNCX2-B16-F1 cells (Supplementary Fig. S1). Overall, these results indicate that $CXCL12_2$ more effectively prevented lung metastasis of CXCR4-expressing melanoma cells than did AMD3100 in a preimplantation model of lung metastasis.

$CXCL12_2$ induces calcium response in CXCR4-expressing B16 cells

We previously showed that $CXCL12_2$ induced CXCR4-mediated calcium response but inhibited chemotaxis in both THP-1 monocytes and HCT116 colorectal cancer cells (6, 7). To confirm that $CXCL12_2$ actively signaled via CXCR4 in CXCR4-B16 cells, we monitored the calcium response induced by 500 nmol/L protein in the presence or absence of 5 μmol/L AMD3100. Both wtCXCL12 and $CXCL12_2$ induced a robust calcium response in CXCR4-B16-F1 cells that was partially inhibited by AMD3100 (Fig. 1F, Supplementary Fig. S2). In contrast, pLNCX2-B16-F1 control cells, that lacked CXCR4, were unable to elicit a response (Supplementary Fig. S2).

$CXCL12_2$ inhibits outgrowth of established CXCR4-B16 metastatic lesions in lung

We next asked if $CXCL12_2$ also prevented the outgrowth of established CXCR4-B16 metastatic lesions in the lung. We previously showed that the CXCL12 cyclic peptide antagonist, T22, was ineffective for inhibiting established tumors (4, 5). CXCR4-B16-F10 cells (4×10^5) were injected intravenously into tail veins and allowed to establish for 5 days. On days 5 and 6, mice were treated intravenously with either 5 μmol/L $CXCL12_2$ or vehicle control (Fig. 2A). Interestingly, tumor burden of $CXCL12_2$-treated mice were significantly less than that of vehicle-treated mice by approximately 50% (Fig. 2B and C). We also found a striking difference in the number of locally invasive lesions in the thoracic cavity of vehicle- versus $CXCL12_2$-treated mice, suggesting that $CXCL12_2$

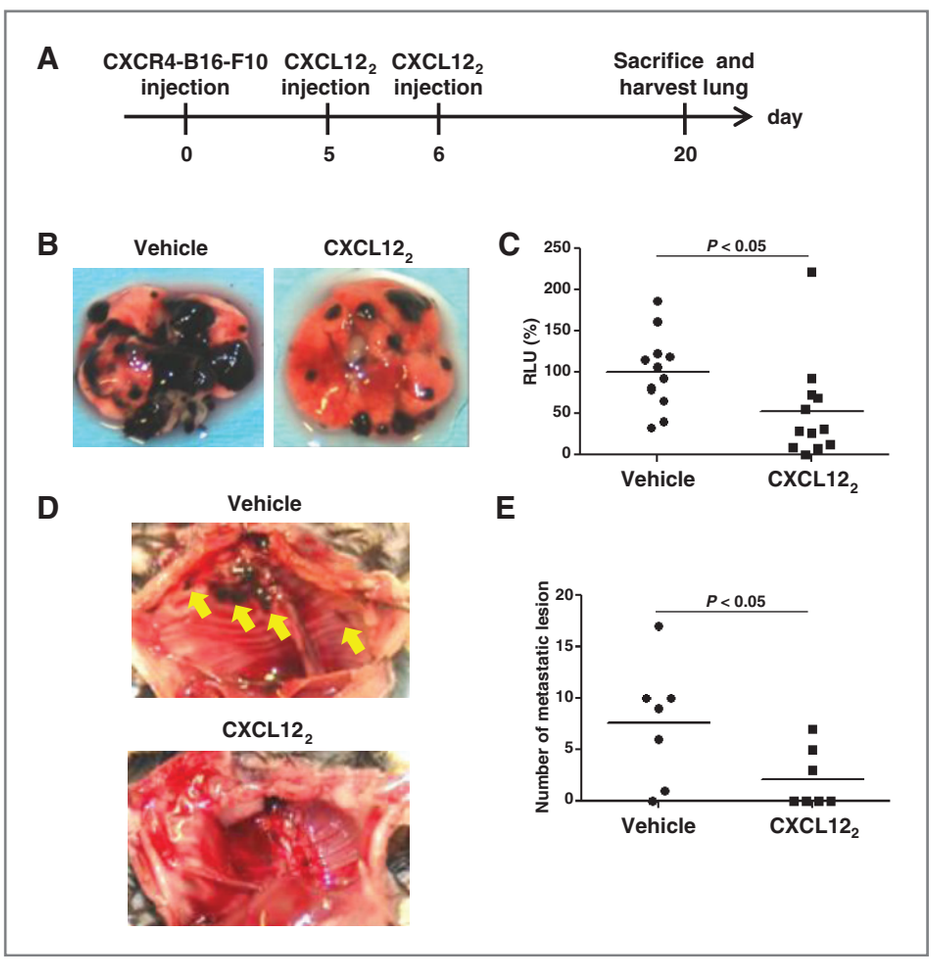

Figure 2. CXCL122 inhibits outgrowth of established CXCR4-B16 metastatic lesions in lung. A, CXCR4-luc-B16-F10 cells (4×10^5) were injected into the tail vein of C57BL/6 mouse, allowed to establish, and then treated with 5 μmol/L $CXCL12_2$ on days 5 and 6. Lungs were harvested 20 days after inoculation, and luciferase activity was measured to evaluate tumor burden. B, representative images of treated and untreated lungs are shown. C, tumor burden in the lungs were quantitatively assessed ($n = 12$; data are a summation of 2 independent experiments). D, representative images of the thoracic cavity wall after lungs were harvested. Yellow arrows indicate tumor invasion. E, the tumor lesions (nodules) invading into the thoracic cavity wall were quantified ($n = 7$; representative of 2 independent experiments with similar results).

Downloaded from http://aacrjournals.org/mct/article-pdf/11/11/2516/2320571/2516.pdf by guest on 15 January 2025

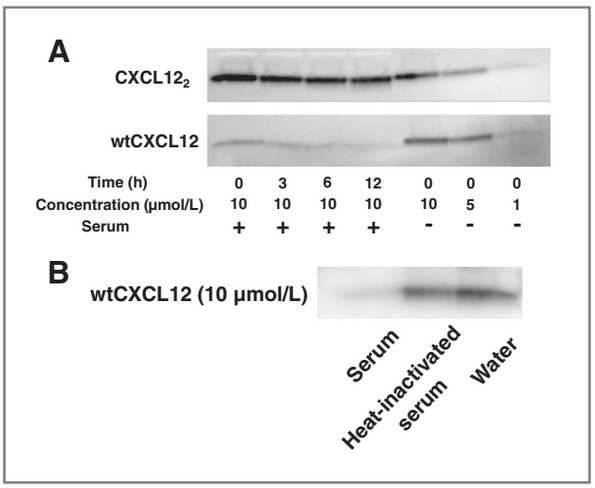

Figure 3. WtCXCL12 is quickly degraded in mouse serum, but CXCL122 is stable for at least 12 hours. A, CXCL122 and wtCXCL12 were incubated with 90% normal mouse serum. Western blot analysis was conducted using anti-hCXCL12 ELISA antibody (R&D Systems ELISA DuoSet). Representative of 2 independent experiments with similar results. B, WtCXCL12 was also incubated with heat-inactivated normal mouse serum and monitored by Western blot analysis. Cropped bands are shown; full-length blots are presented in Supplementary Figs. S3 and S4.

may reduce local metastatic spread (Fig. 2D and E). Taken together, our results suggest that $CXCL12_2$ not only prevents tumor engraftment, but that it also inhibits established pulmonary tumor outgrowth and reduces locally invasive metastatic spread of tumors.

Enhanced m stability of $CXCL12_2$

Next, we sought to explain why dimeric CXCL12 might be a more effective inhibitor *in vivo*. To determine if mouse serum stability was an issue, we incubated 10 μmol/L wtCXCL12 and $CXCL12_2$ in 90% normal mouse serum for up to 12 hours. Western blot analysis using human CXCL12 ELISA detection antibody showed rapid degradation of wtCXCL12 that was consistent with previous reports (Fig. 3A; Supplementary Fig. S3) for full-length blot (11, 18, 19). Surprisingly, $CXCL12_2$ exhibited little degradation after 12 hours incubation. The degradation of wtCXCL12 was abrogated in the presence of heat-inactivated mouse serum (Fig. 3B and Supplementary Fig. S4), suggesting that heat-sensitive enzymes in the mouse serum quickly degraded wtCXCL12 but not $CXCL12_2$.

We used a CXCL12-specific ELISA kit to measure the half-life of wtCXCL12 and $CXCL12_2$ in mouse serum. The pattern of wtCXCL12 and $CXCL12_2$ degradation was similar to that measured by Western blot analysis (Fig. 4A). The degradation of wtCXCL12 was partially blocked by treatment with a protease inhibitor cocktail (Fig. 4B). Nonetheless, the protease inhibitor cocktail did not completely prevent degradation, suggesting that unknown proteins may also degrade wtCXCL12. Alternatively, unknown mouse serum proteins may be binding wtCXCL12 and masking the antibody recognition epitope. The protease inhibitor cocktail did not affect the degradation of $CXCL12_2$ (Fig. 4C), suggesting that some enzymes, which acted upon wtCXCL12, could not degrade $CXCL12_2$.

Functional stability of $CXCL12_2$ in mouse serum

We next asked how long wtCXCL12 remained functional in mouse serum by conducting Transwell chemotaxis assays using THP-1 monocytes. After confirming that chemotaxis buffer containing 1% serum showed no tendency for wtCXCL12 degradation as measured by ELISA (data not shown), we used 10 nmol/L wtCXCL12 in 1% serum as a positive control (labeled as "fresh" in Fig. 4D). Samples of wtCXCL12 were incubated in 90% serum for various time points (0–6 hours). The samples were then diluted to final conditions of 10 nmol/L wtCXCL12 in 1% mouse serum for the chemotaxis experiment. WtCXCL12 gradually exhibited reduced chemotactic activity during incubation with mouse serum and was almost completely inactive after 6 hours (Fig. 4D). Heat-inactivation of serum inhibited the functional degradation of wtCXCL12 (Fig. 4D).

We next asked how long $CXCL12_2$ could be incubated with serum before it was ineffective at inhibiting wtCXCL12-induced chemotaxis. $CXCL12_2$ samples were mixed with 90% mouse serum for the indicated time points (0–24 hours); the samples were then diluted for the chemotaxis assay to final conditions of 10 or 100 nmol/L $CXCL12_2$ in 1% serum containing 10 nmol/L wtCXCL12. $CXCL12_2$ maintained functional inhibition of wtCXCL12-induced migration for up to 24 hours (Fig. 4E). Higher concentrations of $CXCL12_2$ (100 nmol/L) strongly inhibited chemotaxis induced by wtCXCL12 as compared with lower concentrations of $CXCL12_2$ (10 nmol/L; Fig. 4E). $CXCL12_2$ inhibited 10 nmol/L wtCXCL12-induced migration with an $IC_{50} = 19 \pm 6.4$ nmol/L (Supplementary Fig. S5), highlighting the prolonged stability of $CXCL12_2$.

Resistance of $CXCL12_2$ to MMP-2 and DPPIV/CD26 proteases

Segers and colleagues (20) previously showed that a SUMO–CXCL12 fusion protein could be used as a sensitive probe of MMP-2–induced cleavage of the chemokine N-terminus. To monitor N-terminal degradation of wtCXCL12, we generated SUMO-tagged (Smt)-wtCXCL12 and incubated it with mouse serum. Smt-wtCXCL12 degradation in serum was detected by anti-CXCL12 Ab (Fig. 5A; Supplementary Fig. S4 for full-length blot). MMP-2 and DPPIV/CD26 are 2 amino-peptidases that are known to cleave the wtCXCL12 N-terminus at distinct amino acid residues (Fig. 5B). MMP-2 recognizes CXCL12 with its hemopexin C domain and cleaves the peptide bond between Ser4 and Leu5 (10). To test whether or not $CXCL12_2$ possessed enhanced resistance to MMP-2 degradation, 10 μmol/L Smt-CXCL12 and 5 μmol/L Smt-$CXCL12_2$ were incubated with 1.4 ng/μL human MMP-2. Analysis of the time course showed that the half-life of

Downloaded from http://aacrjournals.org/mct/article-pdf/11/11/2516/2320571/2516.pdf by guest on 15 January 2025

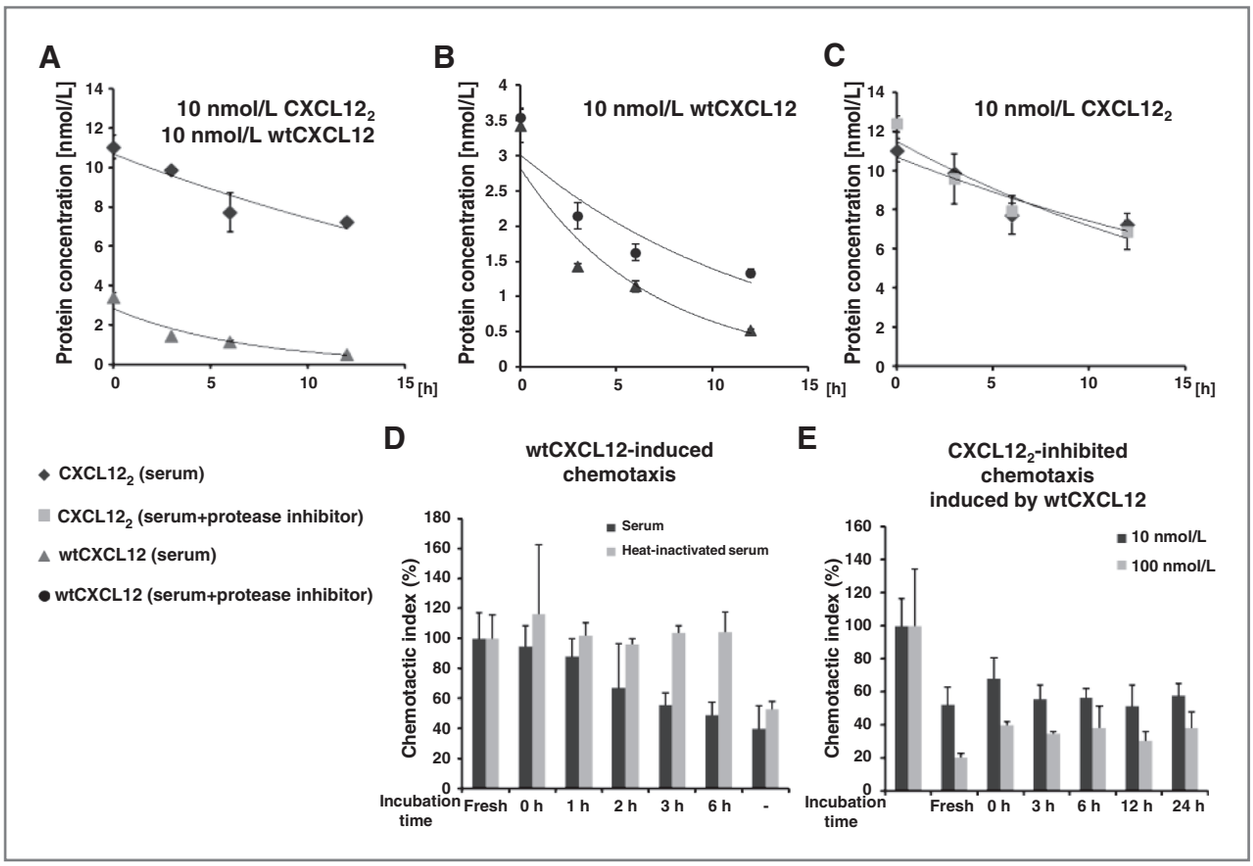

Figure 4. Mouse serum quickly diminishes wtCXCL12 function, whereas CXCL122 remains active for at least 24 hours. A, degradation of 10 nmol/L wtCXCL12 and CXCL12$_2$ was monitored by ELISA in the presence of mouse serum ($n = 3$). Representative of 2 independent experiments with similar results. B, WtCXCL12 (initial starting concentration, 10 nmol/L) degradation monitored in the presence of a protease inhibitor cocktail [cOmplete, Mini, EDTA-free (Roche); $n = 3$]. C, degradation of CXCL12$_2$ (initial starting concentration, 10 nmol/L) was monitored in the presence of protease inhibitors. Negative control (–) contained no chemokine but contained 1% mouse serum ($n = 3$). D, WtCXCL12-induced chemotaxis as a function of time the chemokine is incubated with 90% mouse serum ($n = 3$). E, inhibition of 10 nmol/L wtCXCL12-induced migration by either 10 nmol/L or 100 nmol/L CXCL12$_2$ incubated with 90% mouse serum for indicated time. Chemotaxis assays were conducted using THP-1 monocyte cells ($n = 3$). Negative control (–) contained no CXCL12$_2$ but contained 10 nmol/L wtCXCL12 and 1% mouse serum. As a positive control (fresh), the indicated chemokines were incubated only with 1% mouse serum, which did not result in degradation (data not shown).

CXCL12$_2$ (130 minutes) is twice that of wtCXCL12 (60 minutes; Fig. 5C and D).

DPPIV/CD26 cleaves CXCL12 between Pro2 and Val3 (Fig. 5B; 21) but cannot digest Smt-wtCXCL12 (data not shown). Therefore, we incubated 10 μmol/L wtCXCL12 and 5 μmol/L CXCL12$_2$ with 0.2 ng/μL human DPPIV/CD26 and monitored the degradation of full-length proteins by MALDI-TOF mass spectrometry. For each time point, the intensity of full-length CXCL12 constructs was normalized to a Smt3 internal standard. As was expected, most of wtCXCL12 was cleaved within 1 hour by DPPIV/CD26 with a half-life of 26.5 ± 8.7 minutes. Surprisingly, CXCL12$_2$ was degraded 25-fold more slowly with a half-life of 665 ± 888 minutes (Fig. 5E). In summary, the correlation between N-terminal cleavage and serum-mediated degradation suggests aminopeptidases may be the rate-limiting step for the degradation of full-length CXCL12 and that CXCL12$_2$ may owe its long serum half-life to its resistance to degradation by N-terminal peptidases, such as DPPIV/CD26 and MMP2.

Discussion

CXCR4 and CXCL12 have become a major avenue of cancer research since Muller and colleagues established a role for this chemokine receptor/ligand pair in cancer metastasis (22). CXCR4 is upregulated in at least 23 different cancers (3) and is associated with a clinical poor prognosis (23, 24). We reported that CXCR4 activation upregulates β1 integrin function in B16 melanoma cells, enhancing their ability to adhere to the vessel wall, and thereby increasing the risk for lung metastasis (5). Others reported that CXCR4-CXCL12 signaling also promotes lung metastasis through stromal cells (16, 25). For example, CXCR4 recruits myeloid dendritic cells, which enhance tumor growth, angiogenesis, and micrometastasis (25). Mice with CXCR4$^{+/-}$ stromal cells

Downloaded from http://aacrjournals.org/mct/article-pdf/11/11/2516/2320571/2516.pdf by guest on 15 January 2025

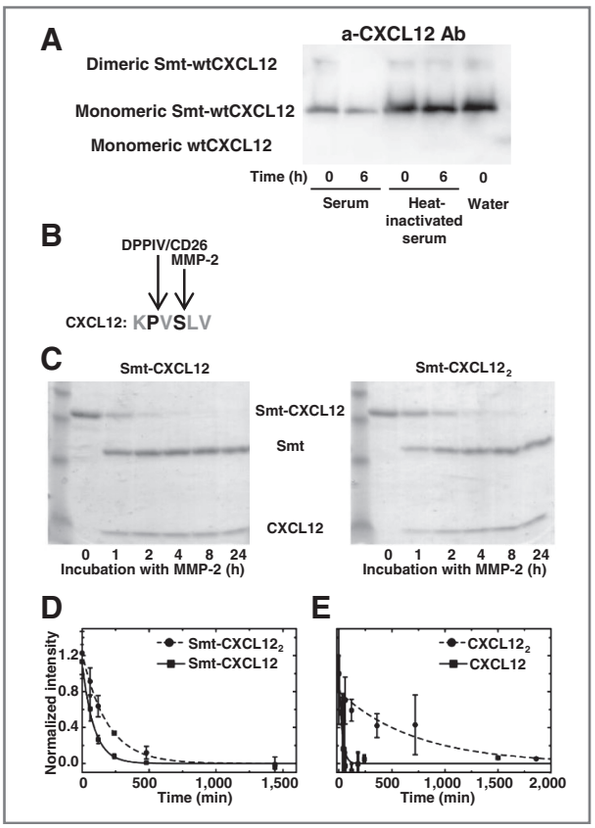

Figure 5. CXCL122 is resistant to both MMP-2 and DPPIV/CD26 cleavage. A, histidine-tagged Smt-wtCXCL12 was incubated with mouse serum and heat-inactivated mouse serum. The Western blot analysis was conducted using an anti-hCXCL12 antibody (R&D Systems ELISA DuoSet). B, MMP-2 cleaves CXCL12 between Ser4 and Leu5, whereas DPPIV/CD26 cuts between Pro2 and Val3. C, cleavage reactions of 10 μmol/L Smt-wtCXCL12 (left) and 5 μmol/L Smt-CXCL12$_2$ (right) in the presence of 1.4 ng/μL human MMP-2 were assessed by reducing SDS-PAGE. Reactions were quenched at the indicated time points and quantified using densitometry to yield half-lives for Smt-wtCXCL12 (61 ± 9 minutes) and Smt-CXCL12$_2$ (129 ± 26 minutes; D). Representative of 2 independent experiments with similar results ($n = 3$). E, 10 μmol/L CXCL12 and 5 μmol/L CXCL12$_2$ were incubated with 0.2 ng/μL human DPPIV/CD26 for the indicated time points and analyzed by MALDI-TOF mass spectrometry. For each mass spectrometry spectra, the intensity of the full-length CXCL12 variants was normalized to an internal Smt3 standard. The half-lives of wtCXCL12 and CXCL12$_2$ were 26.5 ± 8.7 minutes and 665 ± 888 minutes, respectively. Representative of 2 independent experiments with similar results ($n = 3$).

exhibit diminished formation of CXCR4-expressing B16 lung metastasis (16). Administration of AMD3100 to CXCR4$^{+/-}$ mice further reduced tumor formation/growth (16), suggesting that inhibitors of CXCR4 not only control metastatic lung lesions directly, but may also modify the microenvironment.

In contrast to AMD3100, T22, or other CXCR4 antagonists, CXCL12$_2$ is a partial agonist that induces calcium mobilization, but inhibits chemotaxis, actin remodeling, and β-arrestin-2 aggregation in a process we termed "cellular idling" (6). Our finding that CXCL12$_2$ blocked preimplantation inoculation of lung metastases (Fig. 1) may be a result of the dimer's ability to inhibit chemotaxis and actin remodeling, both of which are likely required for metastatic cells to move from the lung endothelium to the lung parenchyma. These effects on cell movement and shape may also explain the ability of the dimer to block local invasion of B16 cells into the chest cavity (Fig. 2). Further studies are warranted to refine the mechanism by which CXCL12$_2$ blocks the metastatic process.

Of note, CXCL12$_2$ treatment also inhibited the growth of 5-day-old established lung tumors. We previously showed that T22 strongly diminished cell metastasis if used in a pretreatment model (i.e., before tumor cell dissemination), but was ineffective at inhibiting the outgrowth of established tumors (5). As increasing evidence supports the role of local CXCR4 expression by stromal cells and immune cells in the establishment and growth of pulmonary metastasis, this suggests that CXCL12$_2$ can potentially influence tumor growth and micrometastasis by affecting both CXCR4$^+$ tumor cells and CXCR4$^+$ stromal cells. On the basis of our current data (Fig. 2D and E), the exciting possibility exists that CXCL12$_2$ can mitigate locally invasive metastatic disease.

Delivery of active compound to the target organ is a major challenge in drug development. In particular, protein- or peptide-based therapies suffer from high rates of serum and liver degradation (26–29). Indeed, CXCL12 and other chemokines have extremely short half-lives in solution (9, 30, 31). Our Western blot analysis, ELISA, and chemotaxis analysis confirmed that wtCXCL12 is quickly degraded in mouse serum, but that CXCL12$_2$ was stable for at least 24 hours. The CXCL12 N-terminus is critical for receptor activation (32) and is cleaved into an inactive form by serum proteases (33). Herein, mass spectrometry revealed that DPPIV/CD26 easily cleaved the N-terminus of wtCXCL12, whereas the rate of CXCL12$_2$ processing was 25-fold slower, suggesting a mechanism for the enhanced serum stability of CXCL12$_2$. MMP-2–mediated cleavage of CXCL12$_2$ was also reduced and showed a 2-fold slower rate of degradation compared with wtCXCL12. Both enzymes are multidomain proteins that rely on first recognizing the structured chemokine domain to orient the N-terminus in the active site of the catalytic domain (10, 20). One possibility is that the enhanced stability of CXCL12$_2$ results from an inability of the enzyme recognition domains to bind dimeric CXCL12, which is a question worthy of further study. Because both DPPIV/CD26 and MMP-2 are secreted in the tumor microenvironment (34), the showed resistance of CXCL12$_2$ to cleavage by these 2 enzymes would predict enhanced stability of CXCL12$_2$ *in vivo*. In addition to MMP-2 and DPPIV/CD26, CXCL12 is recognized by numerous other proteases, such as MMPs 1, 3, 9, 13, and 14 (10), cathepsin G (35), and elastase (36), that are upregulated in the tumor environment of nearly all cancer types (37). Although, treatment with wtCXCL12 would be ineffective under these conditions, CXCL12$_2$ may be much more efficient as a therapeutic agent in the presence of these various proteases.

Downloaded from http://aacrjournals.org/mct/article-pdf/11/11/2516/2320571/2516.pdf by guest on 15 January 2025

In summary, $CXCL12_2$, but not wtCXCL12, strongly inhibited CXCR4-expressing melanoma lung metastasis. Furthermore, $CXCL12_2$ was more effective than AMD3100, the only FDA-approved CXCR4 antagonist (38). Administration of $CXCL12_2$ also reduced the growth of established CXCR4-expressing metastatic lesions. While wtCXCL12 was easily degraded in mouse serum, $CXCL12_2$ had much greater stability, in part due to slower cleavage rates of DPPIV/CD26 and MMP-2. These data support the potential utility of $CXCL12_2$ as therapy for CXCR4-expressing metastatic tumors.

Disclosure of Potential Conflicts of Interest

B.F. Volkman has an ownership interest (including patents) in US Patent 7,923,016. No potential conflicts of interest were disclosed by the other authors.

Authors' Contributions

Conception and design: J.J. Ziarek, B.F. Volkman, S.T. Hwang
Development of methodology: T. Takekoshi, J.J. Ziarek, B.F. Volkman, S.T. Hwang
Acquisition of data (provided animals, acquired and managed patients, provided facilities, etc.): T. Takekoshi, J.J. Ziarek
Analysis and interpretation of data (e.g., statistical analysis, biostatistics, computational analysis): T. Takekoshi, J.J. Ziarek, S.T. Hwang
Writing, review, and/or revision of the manuscript: T. Takekoshi, J.J. Ziarek, B.F. Volkman, S.T. Hwang
Administrative, technical, or material support (i.e., reporting or organizing data, constructing databases): J.J. Ziarek, S.T. Hwang
Study supervision: B.F. Volkman, S.T. Hwang

Acknowledgments

The authors thank Drs. Xuesong Wu and Gyorgy Paragh (Department of Dermatology, MCW) for their advice and technical support.

Grant Support

These studies were supported by Advancing Healthier Wisconsin Research Funds (S.T. Hwang), a MCW/Froedtert Cancer Center Collaborative Research Fellowship (T. Takekoshi), MCW Cancer Center Interdisciplinary Fellowship (J.J. Ziarek), Ann's Hope Foundation for Melanoma (S.T. Hwang), and NIH grant AI058072 (B.F. Volkman).

The costs of publication of this article were defrayed in part by the payment of page charges. This article must therefore be hereby marked *advertisement* in accordance with 18 U.S.C. Section 1734 solely to indicate this fact.

Received May 18, 2012; revised July 16, 2012; accepted July 30, 2012; published OnlineFirst August 6, 2012.

References

1. Ben-Baruch A. The multifaceted roles of chemokines in malignancy. Cancer Metastasis Rev 2006;25:357–71.
2. Sun X, Cheng G, Hao M, Zheng J, Zhou X, Zhang J, et al. CXCL12/CXCR4/CXCR7 chemokine axis and cancer progression. Cancer Metastasis Rev 2010;29:709–22.
3. Dell'Agnola C, Biragyn A. Clinical utilization of chemokines to combat cancer: the double-edged sword. Expert Rev Vaccines 2007;6:267–83.
4. Murakami T, Maki W, Cardones AR, Fang H, Tun Kyi A, Nestle FO, et al. Expression of CXC chemokine receptor-4 enhances the pulmonary metastatic potential of murine B16 melanoma cells. Cancer Res 2002;62:7328–34.
5. Cardones AR, Murakami T, Hwang ST. CXCR4 enhances adhesion of B16 tumor cells to endothelial cells *in vitro* and *in vivo* via beta(1) integrin. Cancer Res 2003;63:6751–7.
6. Drury LJ, Ziarek JJ, Gravel S, Veldkamp CT, Takekoshi T, Hwang ST, et al. Monomeric and dimeric CXCL12 inhibit metastasis through distinct CXCR4 interactions and signaling pathways. Proc Natl Acad Sci U S A 2011;108:17655–60.
7. Veldkamp CT, Peterson FC, Pelzek AJ, Volkman BF. The monomer-dimer equilibrium of stromal cell-derived factor-1 (CXCL 12) is altered by pH, phosphate, sulfate, and heparin. Protein Sci 2005; 14:1071–81.
8. Veldkamp CT, Seibert C, Peterson FC, Volkman BF. Structural basis of CXCR4 sulfotyrosine recognition by the chemokine SDF-1/CXCL12. Sci Signal 2008;1ra4:1–9.
9. Laguri C, Sadir R, Rueda P, Baleux F, Gans P, Arenzana-Seisdedos F, et al. The novel CXCL12gamma isoform encodes an unstructured cationic domain which regulates bioactivity and interaction with both glycosaminoglycans and CXCR4. PLoS ONE 2007;2:e1110.
10. McQuibban GA, Butler GS, Gong JH, Bendall L, Power C, Clark-Lewis I, et al. Matrix metalloproteinase activity inactivates the CXC chemokine stromal cell-derived factor-1. J Biol Chem 2001;276:43503–8.
11. Christopherson KW 2nd, Hangoc G, Broxmeyer HE. Cell surface peptidase CD26/dipeptidylpeptidase IV regulates CXCL12/stromal cell-derived factor-1 alpha-mediated chemotaxis of human cord blood CD34+ progenitor cells. J Immunol 2002;169:7000–8.
12. Tomihari M, Chung JS, Akiyoshi H, Cruz PD Jr, Ariizumi K. DC-HIL/glycoprotein nmb promotes growth of melanoma in mice by inhibiting the activation of tumor-reactive T cells. Cancer Res 2010;70:5778–87.
13. Wiley HE, Gonzalez EB, Maki W, Wu MT, Hwang ST. Expression of CC chemokine receptor-7 and regional lymph node metastasis of B16 murine melanoma. J Natl Cancer Inst 2001;93:1638–43.
14. Feng Y, Broder CC, Kennedy PE, Berger EA. HIV-1 entry cofactor: functional cDNA cloning of a seven-transmembrane, G protein-coupled receptor. Science 1996;272:872–7.
15. De Clercq E. The AMD3100 story: the path to the discovery of a stem cell mobilizer (mozobil). Biochem Pharmacol 2009;77:1655–64.
16. D'Alterio C, Barbieri A, Portella L, Palma G, Polimeno M, Riccio A, et al. Inhibition of stromal CXCR4 impairs development of lung metastases. Cancer Immunol Immunother 2012. [Epub ahead of print].
17. Smith MC, Luker KE, Garbow JR, Prior JL, Jackson E, Piwnica-Worms D, et al. CXCR4 regulates growth of both primary and metastatic breast cancer. Cancer Res 2004;64:8604–12.
18. Davis DA, Singer KE, De La Luz Sierra M, Narazaki M, Yang F, Fales HM, et al. Identification of carboxypeptidase N as an enzyme responsible for C-terminal cleavage of stromal cell-derived factor-1alpha in the circulation. Blood 2005;105:4561–8.
19. Lambeir AM, Proost P, Durinx C, Bal G, Senten K, Augustyns K, et al. Kinetic investigation of chemokine truncation by CD26/dipeptidyl peptidase IV reveals a striking selectivity within the chemokine family. J Biol Chem 2001;276:29839–45.
20. Segers VF, Revin V, Wu W, Qiu H, Yan Z, Lee RT, et al. Protease-resistant stromal cell-derived factor-1 for the treatment of experimental peripheral artery disease. Circulation 2011;123:1306–15.
21. Ohtsuki T, Hosono O, Kobayashi H, Munakata Y, Souta A, Shioda T, et al. Negative regulation of the anti-human immunodeficiency virus and chemotactic activity of human stromal cell-derived factor 1alpha by CD26/dipeptidyl peptidase IV. FEBS Lett 1998;431:236–40.
22. Muller A, Homey B, Soto H, Ge N, Catron D, Buchanan ME, et al. Involvement of chemokine receptors in breast cancer metastasis. Nature 2001;410:50–6.
23. Marechal R, Demetter P, Nagy N, Berton A, Decaestecker C, Polus M, et al. High expression of CXCR4 may predict poor survival in resected pancreatic adenocarcinoma. Br J Cancer 2009;100:1444–51.
24. Sekiya R, Kajiyama H, Sakai K, Umezu T, Mizuno M, Shibata K, et al. Expression of CXCR4 indicates poor prognosis in patients with clear cell carcinoma of the ovary. Hum Pathol 2012;43:904–10.
25. Hiratsuka S, Duda DG, Huang Y, Goel S, Sugiyama T, Nagasawa T, et al. C-X-C receptor type 4 promotes metastasis by activating

Downloaded from http://aacrjournals.org/mct/article-pdf/11/11/2516/2320571/2516.pdf by guest on 15 January 2025

p38 mitogen-activated protein kinase in myeloid differentiation antigen (gr-1)-positive cells. Proc Natl Acad Sci U S A 2011;108: 302–7.

26. Brinckerhoff LH, Kalashnikov VV, Thompson LW, Yamshchikov GV, Pierce RA, Galavotti HS, et al. Terminal modifications inhibit proteolytic degradation of an immunogenic MART-1(27–35) peptide: implications for peptide vaccines. Int J Cancer 1999;83:326–34.

27. Mentlein R, Gallwitz B, Schmidt WE. Dipeptidyl-peptidase IV hydrolyses gastric inhibitory polypeptide, glucagon-like peptide-1(7–36)amide, peptide histidine methionine and is responsible for their degradation in human serum. Eur J Biochem 1993;214: 829–35.

28. Bellmann-Sickert K, Beck-Sickinger AG. Palmitoylated SDF1alpha shows increased resistance against proteolytic degradation in liver homogenates. ChemMedChem 2011;6:193–200.

29. Kluskens LD, Nelemans SA, Rink R, de Vries L, Meter-Arkema A, Wang Y, et al. Angiotensin-(1–7) with thioether bridge: an angiotensin-converting enzyme-resistant, potent angiotensin-(1–7) analog. J Pharmacol Exp Ther 2009;328:849–54.

30. Baggiolini M, Dewald B, Moser B. Interleukin-8 and related chemotactic cytokines–CXC and CC chemokines. Adv Immunol 1994;55: 97–179.

31. Van Zee KJ, Fischer E, Hawes AS, Hebert CA, Terrell TG, Baker JB, et al. Effects of intravenous IL-8 administration in nonhuman primates. J Immunol 1992;148:1746–52.

32. Crump MP, Gong JH, Loetscher P, Rajarathnam K, Amara A, Arenzana-Seisdedos F, et al. Solution structure and basis for functional activity of stromal cell-derived factor-1; dissociation of CXCR4 activation from binding and inhibition of HIV-1. EMBO J 1997;16: 6996–7007.

33. Kanki S, Segers VF, Wu W, Kakkar R, Gannon J, Sys SU, et al. Stromal cell-derived factor-1 retention and cardioprotection for ischemic myocardium. Circ Heart Fail 2011;4:509–18.

34. Bartolome RA, Molina-Ortiz I, Samaniego R, Sanchez-Mateos P, Bustelo XR, Teixido J. Activation of Vav/Rho GTPase signaling by CXCL12 controls membrane-type matrix metalloproteinase-dependent melanoma cell invasion. Cancer Res 2006;66:248–58.

35. Delgado MB, Clark-Lewis I, Loetscher P, Langen H, Thelen M, Baggiolini M, et al. Rapid inactivation of stromal cell-derived factor-1 by cathepsin G associated with lymphocytes. Eur J Immunol 2001; 31:699–707.

36. Valenzuela-Fernandez A, Planchenault T, Baleux F, Staropoli I, Le-Barillec K, Leduc D, et al. Leukocyte elastase negatively regulates stromal cell-derived factor-1 (SDF-1)/CXCR4 binding and functions by amino-terminal processing of SDF-1 and CXCR4. J Biol Chem 2002; 277:15677–89.

37. Egeblad M, Werb Z. New functions for the matrix metalloproteinases in cancer progression. Nat Rev Cancer 2002;2:161–74.

38. DiPersio JF, Uy GL, Yasothan U, Kirkpatrick P. Plerixafor. Nat Rev Drug Discov 2009;8:105–6.

Downloaded from http://aacrjournals.org/mct/article-pdf/11/11/2516/2320571/2516.pdf by guest on 15 January 2025